Turkish J. Eng. Env. Sci.
27 (2003) , 347 – 360.

Geometric Accuracy Testing of Ikonos Geo-Product Mono Imagery Using Different Sensor Orientation Models

Gürcan BÜYÜKSALİH, Murat ORUÇ, Güven KOÇAK
Karaelmas University, Department of Geodesy & Photogrammetry,
67100 Zonguldak-TURKEY
e-mail: buyuksal@karaelmas.edu.tr

Received 31.01.2003

Abstract

This paper addresses the metric accuracy potential of Ikonos Geo imagery for 2D geopositioning. For this, alternative sensor orientation models including rational functions, satellite orbital modelling and terrain relief-corrected affine transformation were used since the Ikonos camera model and the information for external parameters are not provided to the users. Test results arising from the application of these alternative models in a Zonguldak testfield confirm that Ikonos Geo-scenes can yield 2D geopositioning to pixel and in some cases even sub-pixel, accuracy. The paper describes the Zonguldak testfield, discusses geopositioning approaches in the 2D adopted and reports on the geometric accuracy obtained with different sensor orientation models.

Key words: Ikonos Geo-imagery, geometric accuracy testing, rational functions, satellite orbital modelling, terrain relief-corrected affine transformation.

Introduction

Although Ikonos imagery has been commercially available since early 2000, the use of this imagery and especially the scientific investigations on its potential use in various applications have been restricted due to various reasons, related to the closed policy of Space Imaging (SI). Some publications from SI scientists dealt with the radiometric and geometric characteristics of the sensor (Gerlach, 2000), the use of rational polynomial functions as a substitute sensor model (Grodecki, 2001; Dial and Grodecki, 2002a), the 3D mapping accuracy that can be achieved with this imagery using stereo-triangulation with and without ground control (Dial, 2000; Dial and Grodecki, 2002b; Grodecki and Dial, 2002) and investigations into automated road extraction (Dial *et al.*, 2001). On the other hand, independent investigations have mainly focused on the accuracy attainable on digital terrain model (DTM) extraction and ortho-image generation (e.g., Jacobsen, 2001, 2002a, b; Toutin *et al.*, 2001; Toutin and Cheng, 2000; Muller *et al.*, 2001; Davis and Wang, 2001; Vassilopoulou *et al.*, 2002; Baltsavias *et al.*, 2001). In addition, the geopositioning accuracy of Ikonos using 2D transformations and full 3D analysis are also reported by Baltsavias *et al.* (2001), Hanley and Fraser (2001), Fraser *et al.* (2001a, and b) and Fraser *et al.* (2002a, b, c) respectively. Investigations into 3D positioning using alternative models have also been reported by Jacobsen (2001, 2002a, b), Toutin *et al.* (2001), Hu and Tao (2001, 2002) and Tao and Hu (2002a, b).

The basic sensor and mission parameters for the Ikonos-2 satellite are provided at SI's web page (www.spaceimaging.com). Visitors to the site will note that there are basically five products: Geo, Reference, Pro, Precision and Precision Plus. Except for the Geo product, all are ortho-rectified using a DTM, with ground control being required for Precision and Precision Plus ortho-imagery. Absolute planimetric positioning accuracies associated with these categories of imagery are 24, 12, 5, 2 and 1 m, respectively. The error budget for Geo imagery does not include influences due to terrain relief, or possible

additional errors due to projection of the imagery onto an "inflated" ellipsoid at a selected elevation which can be found in the metadata file of the image. Between the Geo and precision products, there are substantial price differences. The accuracy specifications listed would suggest that users of Ikonos images who are seeking the highest metric quality would need to acquire Precision or Precision Plus imagery, which is 5-10 times more expensive than Geo. In June 2001, SI also introduced the Geo Ortho Kit, which provides together with the Geo imagery an Image Geometry Model (IGM) allowing users to generate their own accurate orthoimages using DTMs and ground control points (GCPs). However, this product has a substantially higher cost than normal Geo products (Ortho Kit is currently offered only by SI USA at a 57-78% surcharge and SI Eurasia at a 280% surcharge, while the cheapest Ortho Kit product outside North America is 62 and 98 US$/km^2 for the two SI companies respectively).

Ikonos Geo-imagery has been employed in this investigation, and since the explicit camera model and precise exterior orientation information required to apply conventional collinearity-based models is not provided with Ikonos data, alternative sensor orientation models are needed. The orientation models considered here are rational functions (computed directly from the user-supplied GCPs or implemented as vendor-supplied rational functions coefficients), satellite orbital modelling and terrain relief-corrected affine transformation. These models are running under the Geomatica OrthoEngine V8.2 software package from PCI Geomatics and the Hannover University program system BLASPO. Test results arising from the application of these alternative sensor orientation models within the Zonguldak testfield consisting of high quality GPS-surveyed GCPs are reported in this paper.

Input data and Zonguldak Testfield

Two Ikonos Geo PAN images of the Turkish city, Zonguldak were purchased from SI Eurasia, which is a regional affiliate of SI and is located in Ankara, Turkey. Important characteristics included in the metadata files of these images are given as follows:

While the scene named Image I was acquired in July 2002, Image II was taken in October 2002. These images almost cover the same area on the ground and Image II is shown in Figure 1 with the locations of GCPs. In the upper part of the Ikonos image lies the Black Sea, and other parts of the image include central parts of Zonguldak city which covers a nearly 10 x 10 km area with an elevation range up to 450 m. When the images first received, they were analysed select suitable GCPs for distribution on them uniformly. As a result of this determination, 43 distinct GCPs were measured by GPS survey with an accuracy of about 3 cm. Since these points need to be seen clearly on the images, features such as building corners, crossings were selected. Because of the fine resolution of Ikonos imagery, many cultural features can be identified and used as GCPs.

While the manual measurements of GCPs's image coordinates were carried out by GCP Collection Tool under PCI Geomatica-OrthoEngine software package with zoom factor 4, for the program system BLASPO, sub-program DPLX was used with zoom factor 3. Thus, accuracy of image coordinates of GCPs could be expected in the range of 0.2-0.3 of a pixel.

Geometric Accuracy Test of Ikonos Geo PAN Imagery by PCI Geomatica OrthoEngine V8.2 Software System

The last 15 years have seen various mathematical models formulated for the geometric correction of linear array CCD sensors, especially SPOT, IRS-1

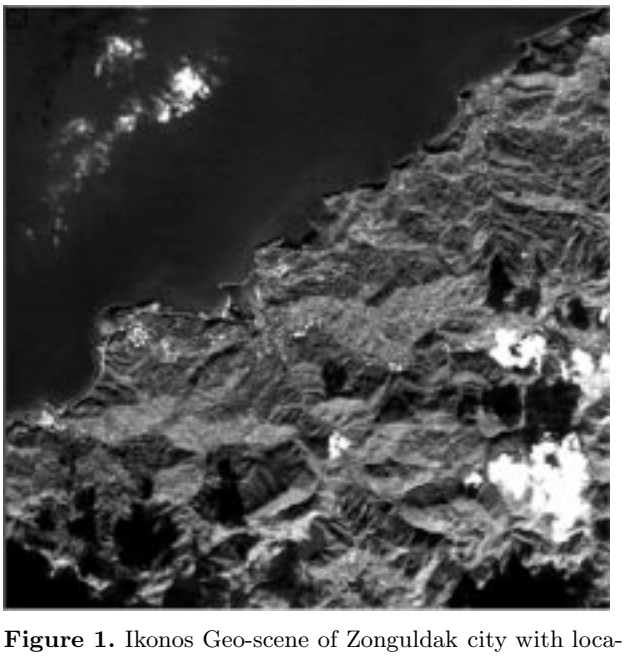

Figure 1. Ikonos Geo-scene of Zonguldak city with locations of GCPs

Characteristics	Ikonos Geo-product PAN images	
	Image I	Image II
Date, Time	02/07/2002, 08:52 GMT	02/10/2002 08:59 GMT
Nominal collection azimuth (deg)	41.2363	10.5023
Nominal collection elevation (deg)	69.6502	63.2446
Sun angle azimuth (deg)	138.2219	166.2923
Sun angle elevation (deg)	67.2403	41.5399
Nadir angle (deg)	20.3498	26.7554
Image size (pixels in row, column)	11,004 x 11,000	11,004 x 11,000
Reference height (m)	206.78	208.04

C/D and MOMS. These models have varying complexity, rigour and accuracy. Strict sensor models have been developed using known sensor information and modified collinearity equations, in some cases including parameters for modelling errors in the interior orientation or in-flight calibration, or incorporating orbital information and orbital constraints. However, for Ikonos, strict models cannot be used, as both the sensor model and ephemeris data are the proprietary information of SI, while raw data are also not commercially available. Thus, alternative models come into play and in this software package two different methods are available to correct Ikonos Geo data: rational functions and satellite orbital modelling. In the following sections, results from the application of these approaches to Geo-product PAN imagery will be explained in detail.

Rational functions

A general model for rational functions, which is appropriate for mono and stereo imaging configurations, is given as

$$x_{ij} = \frac{P_{i1}(X,Y,Z)_j}{P_{i2}(X,Y,Z)_j} \quad , \quad y_{ij} = \frac{P_{i3}(X,Y,Z)_j}{P_{i4}(X,Y,Z)_j} \qquad (1)$$

where

$$P_{i1}(X,Y,Z)_j = a_1 + a_2 \cdot Y + a_3 \cdot X + a_4 \cdot Z + a_5 \cdot Y \cdot X + a_6 \cdot Y \cdot Z + a_7 \cdot X \cdot Z + a_8 \cdot Y^2 + a_9 \cdot X^2 + a_{10} \cdot Z^2 + a_{11} \cdot X \cdot Y \cdot Z + a_{12} \cdot Y^3 + a_{13} \cdot Y \cdot X^2 + a_{14} \cdot Y \cdot Z^2 + a_{15} \cdot Y^2 X + a_{16} \cdot X^3 + a_{17} \cdot X \cdot Z^2 + a_{18} \cdot Y^2 \cdot Z + a_{19} \cdot X^2 \cdot Z + a_{20} \cdot Z^3$$

$$P_{i2}(X,Y,Z)_j = b_1 + b_2 \cdot Y + b_3 \cdot X + b_4 \cdot Z + \cdots + b_{19} \cdot X^2 \cdot Z + b_{20} \cdot Z^3$$

$$P_{i3}(X,Y,Z)_j = c_1 + c_2 \cdot Y + c_3 \cdot X + c_4 \cdot Z + \cdots + c_{19} \cdot X^2 \cdot Z + c_{20} \cdot Z^3$$

$$P_{i4}(X,Y,Z)_j = d_1 + d_2 \cdot Y + d_3 \cdot X + d_4 \cdot Z + \cdots + d_{19} \cdot X^2 \cdot Z + d_{20} \cdot Z^3$$

Here x_{ij},y_{ij} are the normalised (offset and scaled) image coordinates (row,column or line,sample) and X,Y,Z are the corresponding normalised object point coordinates (latitude, longitude and height). Typically, the order of the polynomial P_{ij} is 3, thus leading to 80 rational functions coefficients (RFCs) per image. As can be seen from Eqs. (1), a number of existing restitution algorithms for line scanner imagery are based on special formulations of the ratio-of-polynomials model (e.g., the DLT and polynomial expressions in which the denominator is reduced to unity).

Rational functions have previously found applications in photogrammetry as a restitution model for the real-time loop in stereo photogrammetric workstations, first analytical and then digital (Dowmann and Dolloff, 2000). Until recently, however, their implementation was primarily confined to the defence mapping sector. In the context of Ikonos imagery, RFCs provide a means of reparametrising sensor interior and exterior orientation. This provides a model for extracting 3D information from imagery without explicit reference to either a camera model or satellite ephemeris information. As discussed in Dial *et al.* (2001), Hu and Tao (2001, 2002) and Tao and Hu (2002a, b), RFCs can describe the object-to image-space transformation in "forward" or "inverse" form, and they can be "terrain dependent" or "terrain independent". In terrain independent form, RFCs are supplied for the imagery by SI. They are provided in text format with Ikonos stereo-products, the new Geo Ortho Kit products and also for the

low-cost Geo products. However, in the terrain-dependent approach, RFCs are derived by means of an array of GCPs.

In this study, both terrain dependent and independent forms were evaluated; however, but for the test involving the terrain independent form RFCs were only available for Image II. In the test of terrain dependent form, out of the 43 GCPs, 4 seemed to be erroneous and they were removed. In Table 1, computed root mean square error (rmse) values in X and Y directions are given for each image using different numbers of coefficients. For 3 and 4 RFCs, different GCP/independent check point ICPs configurations were also tested. Using Image I data with the first 3 coefficients, the rmse value for the residual errors was about 12 m in X and 18 m in Y. However, with the addition of a fourth coefficient which takes the elevation values of GCPs into account (see Eq. 1), the rmse values dropped immediately to about 0.6 m X and 0.5 m Y components respectively. Using further terms provided more accurate results, but at the cost of requiring more GCPs in the computation. However, it is interesting to note that differences between the rmse values of 4 and 20 coefficients is only about 0.3 m.

As can be seen from Table 1, at least 6 GCPs are needed to use 3 coefficients of rational functions in OrthoEngine to get accurate results for GCPs. While rmse values increased to about 17 m in X and 21 m in Y for the 6/33 GCPs/ICPs version, they gave very close results for the 7/32 and 8/31 versions. However, with the 15/24 version better rmse values were obtained, though these were still nearly 1.2 times coarser than those produced by a 39/0 version. Figure 2 shows the systematic coordinate biases that resulted from this GCPs/ICPs version with the use of 3 RFCs. In analysis with 4 coefficients, OrthoEngine did not allow the 6/33 version, through the 7/32, 8/31 and 15/24 versions were allowed. While acquired rmse values in the Y direction reached about 2.5 m for the 7/32 version, accuracy values for each component came down to about 1 m for ICPs in the 8/31 version. For the 15/24 version, although the obtained accuracy results in the X and Y directions were about 1.2 times larger than those produced for the 39/0 version, error vectors were becoming smaller and increasingly random (see Fig. 3).

Table 1. The accuracy values for the X and Y components using differents number of RFCs.

Rational functions model with the terrain dependent form utilising GPCs									
		Image I				Image II			
		GCPs		ICPs		GCPs		ICPs	
# Coeff.	# GCPs/ICPs	x-rmse (m)	y-rmse (m)	x-rmse (m)	y-rmse (m)	x-rmse (m)	y-rmse (m)	x-rmse (m)	y-rmse (m)
3	39/0	11.84	18.14	-	-	1.95	32.50	-	-
	5/34	0.00	0.00	15.71	25.81	0.00	0.00	2.39	47.32
	6/33	2.74	0.33	17.05	20.64	0.33	4.01	2.49	37.13
	7/32	2.62	7.67	17.64	21.93	0.35	13.58	2.57	38.79
	8/31	2.57	8.96	17.51	22.48	0.41	15.95	2.72	40.03
	15/24	11.28	16.63	15.06	21.74	1.28	28.94	2.81	38.72
4	39/0	0.65	0.52	-	-	1.12	0.86	-	-
	7/32	0.00	0.00	0.92	2.56	0.00	0.00	1.31	4.17
	8/31	0.26	0.44	1.00	0.95	0.37	0.84	1.82	1.42
	15/24	0.52	0.46	0.86	0.64	0.70	0.56	1.54	1.14
8	39/0	0.58	0.42	-	-	1.01	0.74	-	-
12	39/0	0.51	0.33	-	-	0.89	0.64	-	-
16	39/0	0.49	0.32	-	-	0.76	0.50	-	-
20	39/0	0.36	0.25	-	-	0.54	0.50	-	-
IF ALL GCPs ARE SELECTED IN THE SAME PART OF THE IMAGE									
3	8/31	3.96	6.49	104.11	340.21	1.12	10.42	23.39	1224.25
4	8/31	0.11	0.07	9.58	14.28	1.11	0.53	22.79	11.35

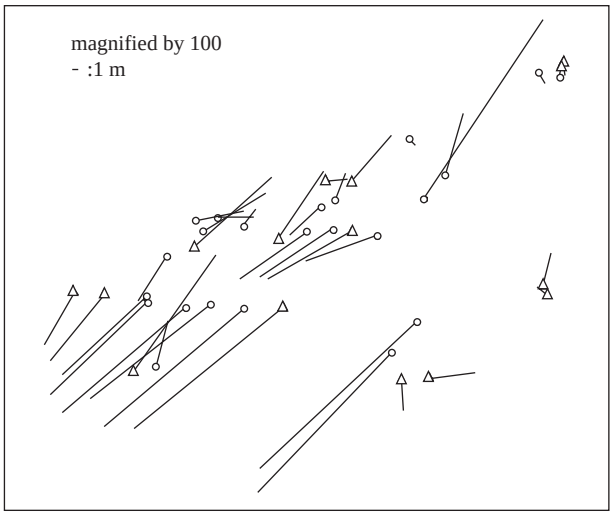

Figure 2. Systematic coordinate biases resulted from the use of the first 3 coefficients of rational functions with a 15/24 GCPs/ICPs configuration for Image I.

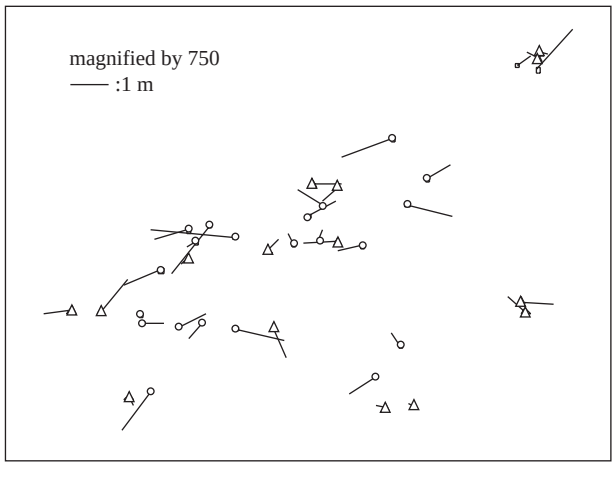

Figure 3. Vector plot of errors for Image I obtained with the addition of fourth RFCs in the 15/24 GCPs/ICPs version.

In addition to the tests with different GCPs/ICPs versions for terrain dependent rational functions, one more test which analyses what happens all the GCPs are selected in the same part of the image was carried out. For Image I, eight GCPs are selected close to each other, and other points were considered ICPs. As can be seen from Table 1, rmse values were acquired about 104 m in X and 340 m in Y for 3 coefficients whereas those values were obtained as 17 m and 22 m in X and Y components respectively in the optimal distribution of 8 GCPs over the image. Applying the fourth coefficient in this condition gave rmse values of about 10 m in X and 14 m in Y. They were equal to almost 1 m for each axis in the optimal 8/31GCPs/ICPs version. Figure 4 shows the error vectors resulted from the use of the unoptimal distribution of 8 GCPs over the Ikonos image. As can be seen from this plot, while the RFCs correct locally at the GCPs, they produce large errors in systematic pattern in areas away from the GCPs.

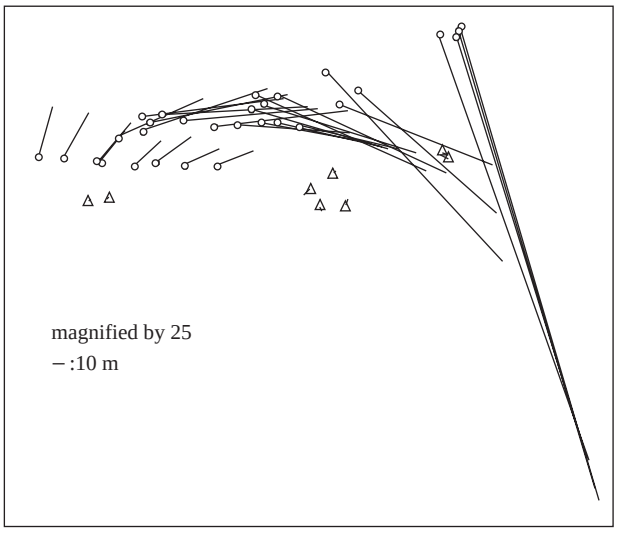

Figure 4. Error vectors obtained by the unoptimal selection of GCPs over an Ikonos image.

For Image II, the same analyses were carried out and the results are also given in Table 1. In this case, a very large rmse value for the X component (≈33 m) was obtained when compared to that of the Y component (≈2 m) using 3 RFCs. As can be seen in Figure 5, a quite systematic pattern in the Y direction resulted over the image. The addition of a fourth coefficient including elevations saw rmse values decrease to about 1.1 m in X and 0.9 m in Y and resulted in a random pattern for error vectors as shown in Figure 6. The same GCPs/ICPs configurations were also analysed for Image II. Although rmse values in the X and Y directions obtained were somewhat larger than those acquired by the 39/0 GCPs/ICPs version, the best results resulted from the use of a 6/33 GCPs/ICPs version for 3 RFCs and a 15/24 version for 4 coefficients. Isolating the GCPs in the same part of the Ikonos image also resulted in large rmse values and error vectors for Image II as well with the use of 3 and 4 RFCs. A vector plot of errors are shown for each case in Fig. 7 and 8 respectively. Rational functions fit locally at GCPs, but not globally.

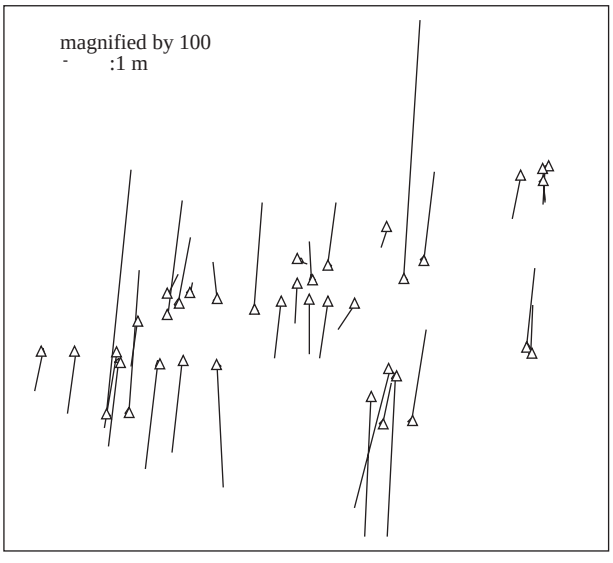

Figure 5. Systematic error pattern especially in Y direction resulted from the use of 3 rational functions coefficients for Image I.

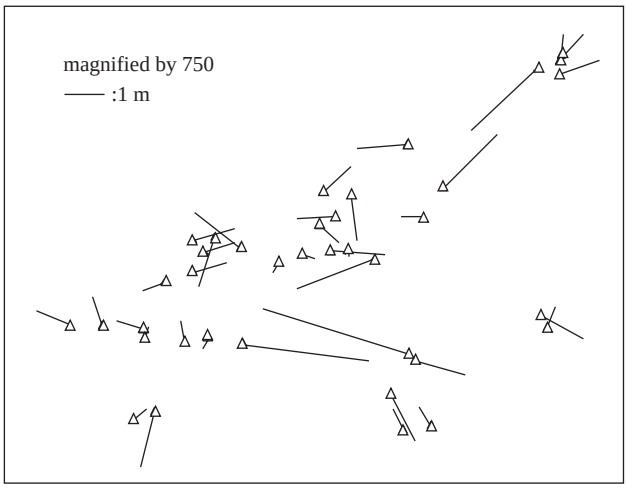

Figure 6. Plot of error vectors resulting from the processing of Image II with 4 RFCs.

In this test of the terrain dependent form of rational functions, OrthoEngine software only allows the user to change the number of coefficients. Therefore, it was not possible to check the reduced and different number of coefficients for the numerator and deminator of rational functions. In addition, possible correlations between the parameters, which are very probable in overparametrised RFCs, could not be checked with the aim of removing some coefficients.

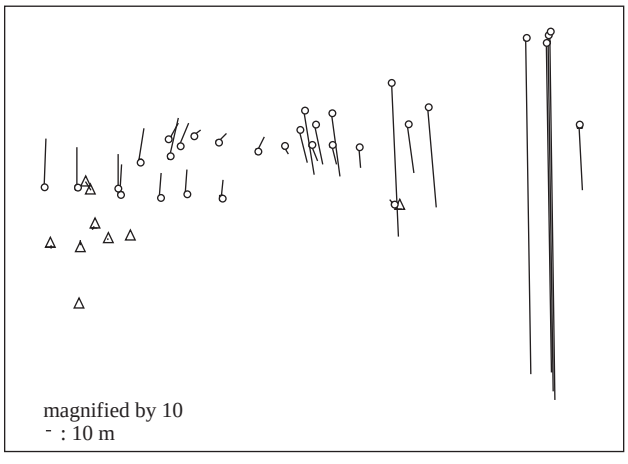

Figure 7. Error vectors resulted with selection of the GCPs in the same part of the Ikonos image.

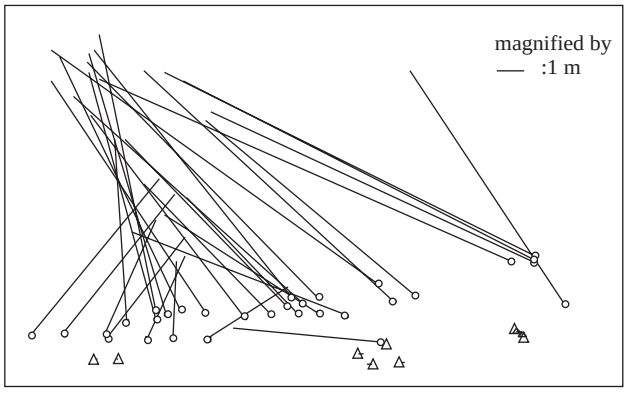

Figure 8. Vector plot of errors obtained by the use of 4 RFCs in the case of unoptimal selection of GCPs over Ikonos Geo imagery.

As mentioned before, RFCs in text format were only available for Ikonos Image II. If an RFCs text file is available, the OrthoEngine will use the terrain independent form and employs the SI Ikonos RFCs block adjustment method in the computation. The RFCs can be directly used for the transformation from object to pixel coordinates. However, the transformation from pixel to object coordinates is an inverse procedure and needs an iterative calculation due to the non-linearity of the RFCs. In this test, 38 of 43 GCPs were used, 5 while GCPs were taken out as blunders. The rmse values were found to be 5.6 m and 0.9 m in the X and Y directions respectively. Vector plots of the errors are included as Figure 9. The quite systematic pattern in the X direction is seen in the image. Using only 4 GCPs in the computation increased the rmse values at the remaining check points to 6.6 m in X and 1.1 m in

Y. Other GCPs/ICPs versions did not change the results significantly and rmse values, especially in the Y direction, became unchanged between the different GCPs/ICPs configurations.

Satellite orbital modelling

The Ikonos model in the PCI Geomatica OrthoEngine was developed first for multi-sensor images at the Canadian Centre for Remote Sensing (CCRS) and given by Toutin (1995) and then adopted to high-resolution images (Toutin and Cheng, 2000; Toutin *et al.*, 2001). As has been stated in OrthoEngine manuals and the cited studies, the proprietary sensor model of this software utilises the basic information available from the metadata and image files. For example, approximate sensor viewing angles can be computed using the nominal collection elevation and azimuth in addition to the nominal ground resolution. It further reflects the physical reality of the complete viewing geometry and corrects all the geometric distortions due to the platform, sensor and Earth that occur during the imaging process, and also any deformations of the cartographic projection.

Table 2 gives the rmse values obtained by the application of satellite orbital modelling for each image. For Image I, geometric correction led to an rmse of 1.48 m and 0.58 m in the X and Y axes respectively. Vector plots of the errors show a highly systematic pattern, especially in the X component (see Fig. 10). In addition to using all GCPs in the computation, some of them were assigned as ICPs and used in the test. For the 15/24, 8/31, 7/32 and 6/33 GCPs/ICPs versions, while change in the Y-rmse remains small, it was prominent in the rmse value of the X component. We also checked the 5/34 and 4/35 versions, but blundered results were obtained for the X and Y directions. For Image II, the resultant error vectors (see Fig. 11) do not have a systematic pattern in the X direction as in Image I; a more random representation was obtained with smaller rmse values for the X component. When the 15/24 GCPs/ICPs version is employed, the rmse value increases nearly 1.4 times compared to that of the 39/0 version. However, when the 8/31, 7/32 and 6/33 GCPs/ICPs configurations were used, better rmse values in X against Y were obtained compared to those of the 15/24 version. The OrthoEngine satellite orbital modelling approach was also tested with the use of only 4 and 5 GCPs for Image II, as happened with Image I, very large rmse values for the remaining check points were obtained.

Hannover University Program System-BLASPO

The program BLASPO is a supplement for well-known program system BLUH of Hannover University. It is a bundle adjustment program developed for linear array pushbroom scanner images like SPOT, IRS-1C/1D and MOMS. After Ikonos Geo-scenes became available for users 2 sub-programs, CORIKON and RAPORI, were written to handle this type of data. While CORIKON uses terrain relief-corrected affine transformation for the geometric correction of Ikonos Geo-scenes (Jacobsen

Table 2. The accuracy values resulting from PCI OrthoEngine satellite orbital modelling using different GCPs/ICPs configurations for Images I and II.

PCI Geomatica OrthoEngine satellite orbital modelling approach								
	Image I				Image II			
	GCPs		ICPs		GCPs		ICPs	
# GCPs/ICPs	x-rmse (m)	y-rmse (m)	x-rmse (m)	y-rmse (m)	x-rmse (m)	y-rmse (m)	x-rmse (m)	y-rmse (m)
39/0	1.48	0.58	-	-	1.15	0.88	-	-
15/24	1.66	0.59	1.80	0.68	0.77	0.57	1.66	1.11
8/31	0.50	0.38	3.77	0.82	0.39	0.86	1.37	1.67
7/32	0.25	0.40	5.85	0.81	0.08	0.51	1.43	1.99
6/33	0.00	0.02	7.69	1.07	0.00	0.16	1.60	1.78
5/34	0.03	0.00	96.85	1.47	168.10	100.08	797.58	85.48
4/35	611.01	838.05	488.01	475.59	605.11	847.78	480.79	483.88

2001, 2002a, b), RAPORI implements the terrain independent form of rational functions with vendor-supplied RFCs. The underlying theory of these programs, along with results from their implementation, will be explained step by step in the following sections.

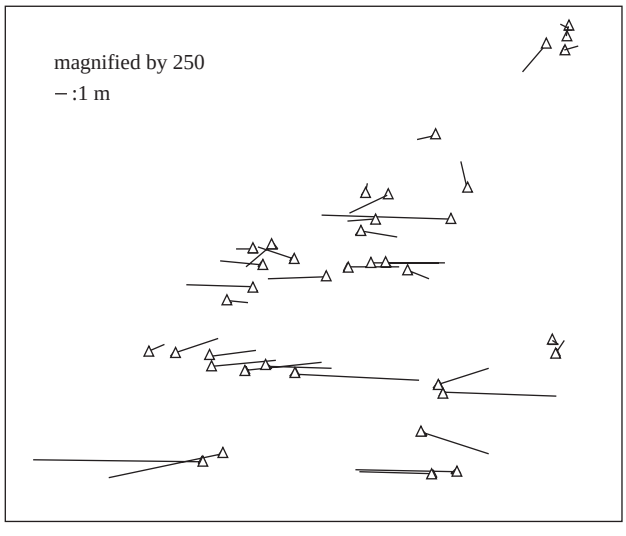

Figure 9. Error vectors resulted from the use of text format and vendor-supplied RFCs.

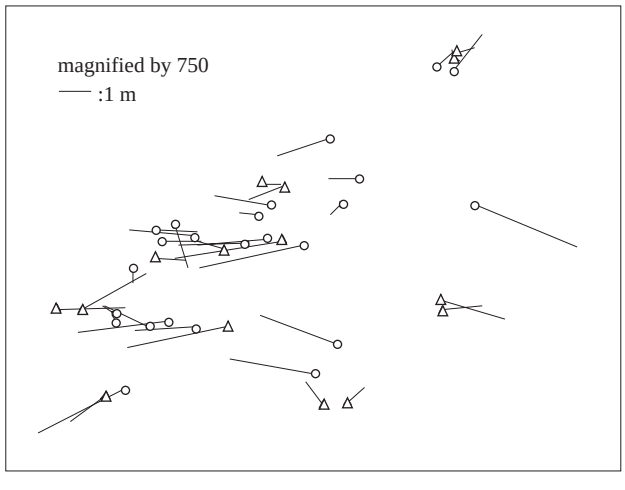

Figure 10. Vector plot of the errors resulting from the use of satellite orbital modelling for Image I.

Terrain relief-corrected affine transformation using CORIKON

The input data for CORIKON include the object coordinates and geocoded values of image coordinates of GCPs. Image coordinates measured by the subprogram DPLX in pixels should first be converted to the ground system by another sub-program, MANI, using the Ikonos Geo image's metadata file which is provided with. a tfw or .hdr extension. For this geometric construction, nominal collection elevation and the nominal collection azimuth values included in the header data are sufficient. Then, discrepancies between object and geocoded image coordinates of GCPs are computed. For Image I, the mean square differences of ±17.55 m and ±24.54 m in the X and Y directions were obtained respectively. However, in this case, the positions directly determined with the Geo-scene are influenced by relief displacement and also a remaining scene orientation error. In this case, at the first step, object coordinates should be corrected by relief displacement (dL in Fig. 12) using the nominal collection elevation and azimuth values given in the metadata file. Then, simple affine transformation will only be required to relate object and image space. Terrain relief-correction will lead to changes in the planimetric X and Y coordinates of GCPs according to Eqs. (2):

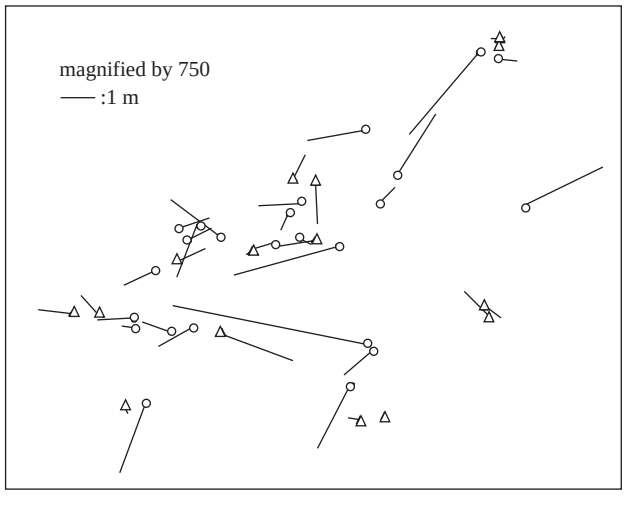

Figure 11. Error vectors obtained by the use of satellite orbital modelling approach for Image II.

$$\begin{aligned} \Delta X &= -(Z - Z_0)\sin a/\tan e \\ \Delta Y &= -(Z - Z_0)\cos a/\tan e \end{aligned} \qquad (2)$$

where Z is the height of a given ground point, Z_0 the height of the reference plane, a the sensor azimuth, e the sensor elevation and ΔX and ΔY the planimetric displacements.

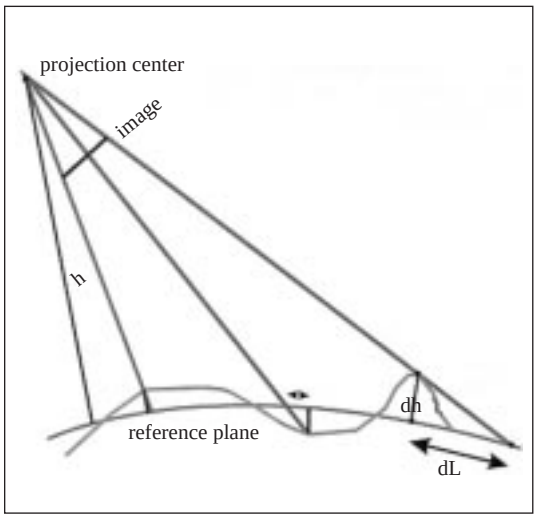

Figure 12. Effect of terrain relief for the Ikonos Geo-scene acquisition.

The terrain relief-correction and the affine transformation are combined in a single operation in CORIKON involving eight parameters given as Eqs. 3:

$$\begin{aligned} x &= a_1X + a_2Y + a_3Z + a_4 \\ y &= a_5X + a_6Y + a_7Z + a_8 \end{aligned} \tag{3}$$

This operation is called terrain relief-corrected affine transformation. The results for Images I and II are summarized and given in Table 3. For Image I, it showed large errors occurring in the X direction at all the image points. The rmse values were found to be ±5.27 m and ±0.83 m in the X and Y directions respectively. Vector plot for errors (see Fig. 13) resulted in a systematic error pattern lying along the East-West direction in the Geo-scene. When looking at the coefficients of affine transformation, the major correction needed seems to be shifts (-9952.89 and -8491.20) between the 2 spaces. The 2 scale and shear terms are required to model smaller deviations between 2 spaces. It was found out that the 2 scale terms (0.997340 and 1.001844) deviated from unity in the third decimal place only. Also, the nonorthogonality coefficients ranging from 0.000092 to 0.0024 were obtained.

It is also worth noting that program CORIKON is identifying and respecting the blunders in an online fashion based on data-snooping technique using Baarda method. Based on a sigma apriori of 1.5 m, four GCPs were determined as blunders by the program and taken out in this implementation.

In CORIKON it is also possible to estimate the approximate values for nominal collection azimuth and elevation. The use of CORIKON resulted in azimuth and elevation values of 394.3403° and 72.3310° respectively for Image I. These estimated values produced 6.90° (41.2363°-34.3403°) and 2.68° (72.3310°-69.6502°) discrepancies from the original

Table 3. Accuracy values from the use of Hannover University program CORIKON for Images I and II.

Terrain relief-corrected affine transformation by CORIKON									
		Image I				Image II			
		GCPs		ICPs		GCPs		ICPs	
# GCPs/ICPs	Ineration number	x-rmse (m)	y-rmse (m)	x-rmse (m)	y-rmse (m)	x-rmse (m)	y-rmse (m)	x-rmse (m)	y-rmse (m)
39/0	1st iter.	5.27	0.83	-	-	4.95	1.00	-	-
	2nd iter.	1.14	1.17	-	-	1.18	1.00	-	-
15/24	1st iter.	5.10	0.79	-	-	3.83	0.85	-	-
	2nd iter.	0.92	1.40	1.39	1.35	0.43	0.76	1.52	1.48
8/31	1st iter.	3.09	0.81	-	-	2.54	1.17	-	-
	2nd iter.	0.40	0.85	1.22	1.05	1.17	1.24	1.76	1.10
6/33	1st iter.	2.98	0.73	-	-	2.49	0.77	-	-
	2nd iter.	0.31	0.91	1.21	1.08	0.80	0.80	1.77	1.02
5/34	1st iter.	1.72	0.72	-	-	1.92	1.22	-	-
	2nd iter.	0.31	0.58	2.14	1.12	0.35	1.20	3.61	1.08
4/35	1st iter.	7.15	6.27	-	-	7.00	5.71	-	-
	2nd iter.	2.39	3.97	2.63	3.54	2.20	4.34	4.10	4.60

values given in the metadata file. These changes seem to be very large but the reason behind them remains unknown to us at present. When the estimated values were used instead of the original values in the CORIKON implementation, the terrain relief-corrected affine transformation gave rmse values of 1.15 m in X and 1.17 m for Y. The error vectors (see Fig. 14) resulting from this run show that there was no remaining systematicity along the East-West direction in the image.

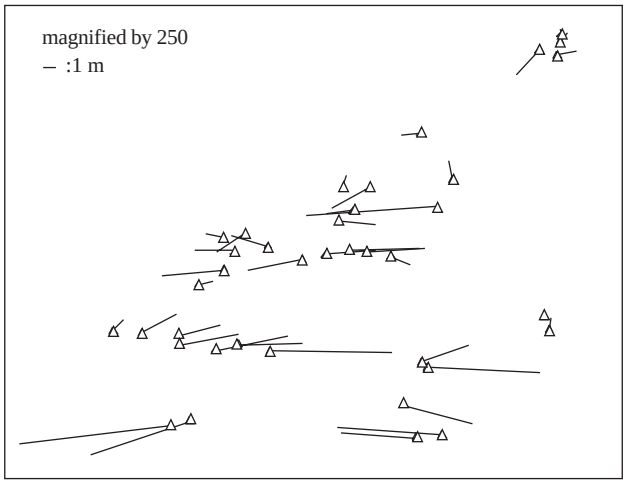

Figure 13. Systematic error pattern in the X direction from the use of terrain-relief corrected affine transformation for Image I.

As can be seen from Table 3, different GCPs/ICPs configurations were also tested for Image I. Using only 4 GCPs produced rmse values of about 2.6 m X and 3.5 m for Y. With the application of the 5/34 version, accuracy results of about 2 m and 1 m were acquired for the X and Y components respectively. However, the 6/33 and 8/31 versions provided rmse values of 1.2 m for X and 1.1 m for Y, which are quite similar to those obtained by the 39/0 version. Finally, the use of 15 GCPs distributed uniformly over an Ikonos image gave rmse values of about 1.4 m in each direction for the remaining check points.

The same procedure was also applied to Image II. CORIKON provided rmse values of 13.67 m and 19.78 m for the X and Y directions respectively for the uncorrected coordinate differences. When the terrain relief-corrected affine transformation was used, the error values dropped to 4.95 m for X and 1.00 m for Y. As happened with Image I, large rmse values occurred in the X direction for Image II. Plot of error vectors (see Fig. 15) resulting from the use of relief correction and affine transformation showed a systematic pattern in an East-West direction. CORIKON once again gave the estimated azimuth and elevation values of 2.8380° and 64.2430°. They resulted in 7.66° (10.5023°-2.8380°) and 1.00° (64.2430°-63.2446°) discrepancies between the original and estimated values. The use of estimated nominal collection azimuth and elevation values provided a significant change in the magnitude of rmse values in an X direction. Error vectors are plotted in Figure 16 and display a highly random pattern, although the overall dimensions of the rmse values are very close to 1 m in each direction.

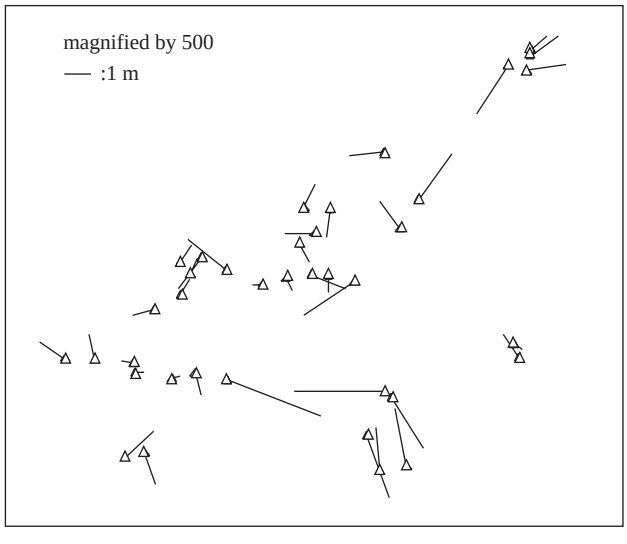

Figure 14. Vector plot of the errors computed using the estimated nominal collection azimuth and elevation values in CORIKON implementation.

Analyses with GCPs/ICPs configurations used for Image I were also performed for Image II. However, as can be seen from Table 3, in the 6/33 and 8/31 versions rmse values of about 1.8 m for X and 1.1 m for Y were obtained. While the accuracy value in Y remained stable, change in the X direction was about 0.5 m when compared with the rmse values of the 39/0 version. The same comment can be made for the 5/34 version, while the Y-rmse value obtained was around 1.1 m, it was about 3.6 m for X component. For Image II, the 4/35 GCPs/ICPs version gave the coarsest accuracy values of 4.1 m and 4.6 m in the X and Y directions respectively. For the 15/24 version, an rmse value of 1.5 m was obtained for both X and Y components.

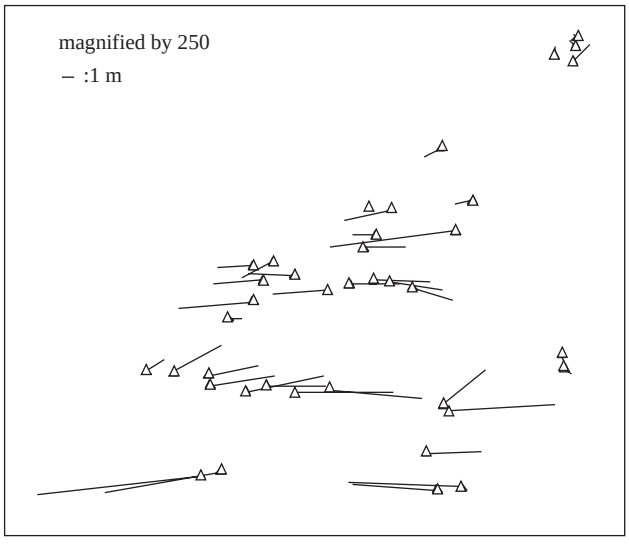

Figure 15. Systematic pattern of error vectors in X direction obtained using terrain relief-corrected affine transformation for Image II.

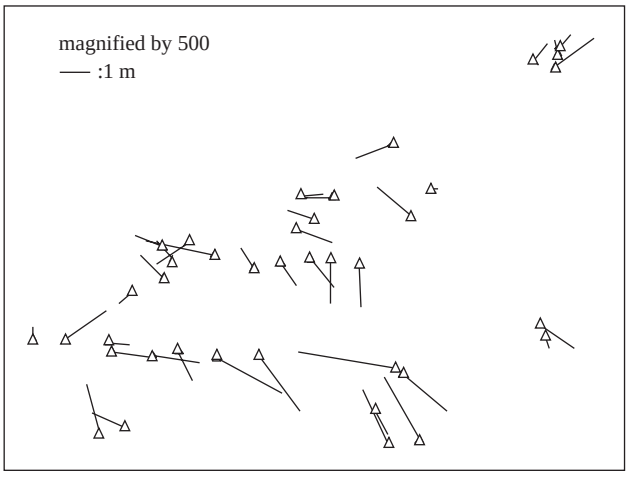

Figure 16. Error vectors in random pattern resulting from the use of nominal collection azimuth and elevation values estimated by CORIKON for Image II.

Accuracy test using vendor-supplied RFCs RAPORI

Image II was handled with RAPORI based on the available RFCs. The 80 RFCs supplied with the imagery along with 10 scale and offset terms are used for object to image transformation. The obtained accuracy values were 5.53 m for X and 0.88 m for Y. A plot of error vectors is also given in Figure 17. The results are very close to those achieved by CORIKON implementation (directly based on the original nominal collection elevation and azimuth and PCI Geomatica OrthoEngine software process with the vendor-supplied text format RFCs).

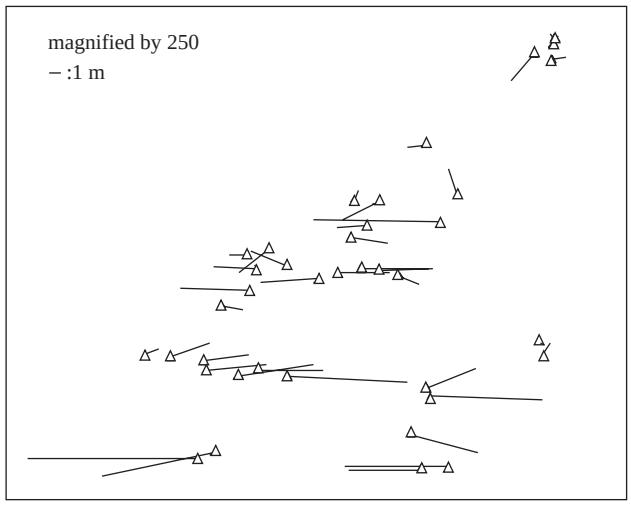

Figure 17. Vector plot of errors obtained by RAPORI using vendor-supplied RFCs for Image II.

Discussion

Our investigation has shown that Ikonos Geo imagery has the potential to yield a pixel, in some cases even sub-pixel, accuracy for 2D geopositioning. Furthermore, this high level of accuracy can be obtained with a small number of control points, say 6 to 8 GCPs, in a Zonguldak testfield with a height range of about 500 m and an undulating surface structure. The results of 2D accuracy analysis are also confirmed by Hanley and Fraser (2001) who demonstrated that rmse positioning accuracies of 0.3-0.5 pixel were obtained with 6 GCPs and 20-25 ICPs. In addition, testing by Baltsavias *et al.* (2001) demonstrated that a single Ikonos image can readily yield an XY positioning accuracy of 0.5 pixel or better. These highly accurate geopositioning results were obtained over the Ikonos image of the very flat Melbourne testfield with only 80 m height differences. As regards alternative sensor orientation models, it has been shown that rational functions with 6 coefficients provide the best results. However, in this model, the estimation of RFCs using GCPs needs many control points that cover the entire planimetric and height range of the scene and this can be very difficult to achieve in practise, as well as being costly. Rational functions can also

lead to severe extrapolation errors and possible undulations between GCPs. The results acquired by terrain-dependent RFCs compare very favourably to the 1-2 m planimetric accuracy reported by Grodecki and Dial (2002), Fraser *et al.* (2002) and Hu and Tao (2001). Toutin and Cheng (2000) also tested rational polynomials and reached accuracies of about 2 m for X and 5 m for Y using only 7 GCPs and 23 ICPs. On the other hand, the use of terrain-independent form of vendor-supplied RFCs produced larger rmse values (5.6 m) the X direction while Y-rmse (0.9 m) was still obtained in the submeter level. Although the accuracy value in Y coincides with the results provided using terrain independent text format RFCs document in other studies (Tao and Hu, 2002a, b), the reason behind the coarse result in the X direction is still unknown. The same comment can also be made for the terrain relief-corrected affine transformation available with the Hannover University program CORIKON using the original nominal collection elevation and azimuth values. It gave very similar accuracy figures acquired by vendor-supplied RFCs. Still larger rmse values in an X direction a showing quite systematic pattern in an East-West direction of Geo-scene commonly resulted from these methods. However, the estimation of nominal collection azimuth and elevation values by CORIKON removed systematic error in the X direction, and thus the same level of accuracy with the Y component was obtained. The changes between original and estimated nominal collection azimuth and elevation values are prominent and no answer in presently available for this matter. CORIKON was also applied to the several other datasets (see Jacobsen, 2001, 2002a, b). The accuracy results obtained were in the range 1-4 pixels. Coarse results from this method were acquired in a testfield containing steep slopes and large height differences. PCI satellite orbital modelling produced, especially for Image II, larger rmse values for X while submeter accuracy was obtained for the Y direction. This model was tested by other users (Toutin *et al.*, 2001, Baltsavias *et al.*, 2001) as well, and these works also arrived at the same conclusion of larger rmse values in the X direction of up to 6 pixels depending upon the dataset itself. This means that the method does not propagate very well in the X direction.

Conclusions

SI's high-accuracy level products, e.g., Precision and Precision Plus, can be difficult to generate outside some countries (requiring GCPs and DEM from the users) and are otherwise expensive. However, the low-cost and base-level product Ikonos Geo imagery can be processed and orthorectified by simple mathematical models in a users's operational environment. The findings presented in this paper for 2D geopositioning from Ikonos Geo-product data using such models illustrate that high accuracy is really possible. The investigation has also confirmed that with a straightforward translation of object point coordinates produced via RFCs, accuracies at the submetre level rather than the specified 24 m absolute accuracy level can be expected. Perhaps of most practical significance is the fact that 2D geopositioning to pixel, in some cases sub-pixel, accuracy can be achieved by these alternative models with a minimum number of GCPs. However, both the parametric model from PCI and model based on terrain relief-corrected affine transformation implemented by CORIKON did not propagate very well in the X direction, while both models yield sub-metre accuracy in the Y direction. The reason for this problem is difficult to discern. However, we are suspicious about the nominal collection elevation and azimuth values supplied to users in the metadata file of Ikonos Geo imagery.

Acknowledgements

This work was carried out under a project supported through the cooperation of TÜBİTAK-JULICH, code No. 101Y090.

References

Baltsavias, E., Pateraki, M. and Zhang, L., "Radiometric and geometric evaluation of Ikonos Geo images and their use for 3D building modelling". Proc. Joint ISPRS Workshop "High Resolution Mapping from Space 2001," Hannover, 19-21 September. Institute of Photogrammetry & Geoinformation, University of Hannover, 21 (on CD ROM), 2001.

Davis, C.H. and Wang, W., "Planimetric accuracy of Ikonos 1 m panchromatic image products". Proc. ASPRS Annual Conference, St. Louis, 23-27 April. American Society of Photogrammetry & Remote Sensing, 14 (on CD ROM), 2001.

Dial, G., "Ikonos satellite mapping accuracy". Proc. ASPRS Annual Conference, Washington, DC, 22-26

May. American Society of Photogrammetry & Remote Sensing, 8 (on CD ROM), 2000.

Dial, G., Gibson, L. and Poulsen, R., "Ikonos satellite imagery and its use in automated road extraction". In Baltsavias, E., Gruen, A., Van Gool, L. (eds.), Automated Extraction of Man-Made Objects from Aerial and Space Images (III), Balkema Publishers, Lisse, 357-367, 2001.

Dial, G. and Grodecki, J., "Block adjustment with rational polynomial camera models". Proc. ACSM-ASPRS 2002 Annual Conference, Washington, DC, April 22-26, 17 (on CD ROM), 2002a.

Dial, G. and Grodecki, J., "Ikonos accuracy without ground control". Proc. of ISPRS Commission I, Mid-Term Symposium, Denver, CO, November, 10-15, 2002b.

Dowmann, I. and Dolloff, J.T., "An evaluation of rational functions for photogrammetric restitution". Int. Arch. Photogramm. Remote Sens. 33(B3/1), 252-266, 2000.

Fraser, C.S., Hanley, H.B. and Yamakawa, T., "Sub-metre geopositioning with Ikonos Geo imagery". Proc. Joint ISPRS Workshop "High Resolution Mapping from Space 2001," Hannover, 19-21 September. Institute of Photogrammetry & Geoinformation, University of Hannover, 8 (on CD ROM), 2001a.

Fraser, C.S., Baltsavias, E. and Gruen, A., "3D building reconstruction from high-resolution Ikonos stereo images". 3rd Int. Symposium on Automated Extraction of Man-Made Objects from Aerial and Space Images, Ascona, Switzerland, June 10-15, 13, 2001b.

Fraser, C.S., Hanley, H.B. and Yamakawa, T., "Three-dimensional positioning accuracy of Ikonos imagery". Photogramm. Rec. 17(99), 465-479, 2002a.

Fraser, C.S., Hanley, H.B. and Yamakawa, T., "High-precision geopositioning from Ikonos satellite imagery". Proc. ASPRS Annual Conference, Washington, DC, 22-26 May. American Society of Photogrammetry & Remote Sensing, 9 (on CD ROM), 2002b.

Fraser, C.S., Baltsavias, E. and Gruen, A., "Processing of Ikonos imagery for submetre 3D positioning and building extraction". ISPRS Journal of Photogrammetry & Remote Sensing 56, 177-194, 2002c.

Gerlach, F., "Characteristics of space imaging's one-meter resolution satellite imagery products". Int. Arch. Photogramm. Remote Sens. 33(B1), 128-135, 2000.

Grodecki, J., "Ikonos stereo feature extraction – RPC approach". Proc. ASPRS Annual Conference, St. Louis, 23-27 April. American Society of Photogrammetry & Remote Sensing, 7 (on CD ROM), 2001.

Grodecki, J. and Dial, G., "Ikonos geometric accuracy validation". Proc. of ISPRS Commission I, Mid-Term Symposium, Denver, CO, November, 10-15, 2002.

Hanley, H.B. and Fraser, C.S., "Geopositioning accuracy of Ikonos imagery: indications from 2D transformation". Photogramm. Rec. 17(98), 317-329, 2001.

Hu, Y. and Tao, V., "3-D reconstruction algorithms with the rational function model and their applications for Ikonos stereo imagery". Proc. Joint ISPRS Workshop "High Resolution Mapping from Space 2001," Hannover, 19-21 September. Institute of Photogrammetry & Geoinformation, University of Hannover, 12 (on CD ROM), 2001.

Hu, Y. and Tao, V., "Updating solutions of the rational function model using additional control information". Photogrammetric Engineering & Remote Sensing, 68, 715-723, 2002.

Jacobsen, K., "Automatic matching and generation of orthophotos from airborne and spaceborne line scanner images". Proc. Joint ISPRS Workshop "High Resolution Mapping from Space 2001," Hannover, 19-21 September. Institute of Photogrammetry & Geoinformation, University of Hannover, 9 (on CD ROM), 2001.

Jacobsen, K., "Generation of Orthophotos with Carterra Geo Images without Orientation Information". ASPRS annual convention, Washington, 9, CD-ROM, 2002a.

Jacobsen K., "Mapping with IKONOS images". 22nd EARSeL Symposium, Prague, 8, 2002b.

Muller, J.P., Kim, J.R. and Tong, L., "Automated mapping of surface roughness and landuse from simulated and spaceborne 1 m data". In Baltsavias, E., Gruen, A. and Van Gool, L. (eds.), Automated Extraction of Man-Made Objects from Aerial and Space Images (III), Balkema Publishers, Lisse, 369-379, 2001.

Tao, V., Hu and Y., "3D reconstruction methods based on the rational function model". Photogrammetric Engineering & Remote Sensing, 68, 705-714, 2002a.

Tao, V. and Hu, Y., "Photogrammetric explotation of Ikonos imagery using the rational function model". Proc. ACSM-ASPRS 2002 Annual Conference, Washington, DC, April 22-26, 12 (on CD ROM), 2002b.

Toutin, Th., "Multisource data fusion with an integrated and unified geometric modelling". EARSel advances in remote sensing, 4(2-X), 118-129, 1995.

Toutin, Th., Cheng, P., Demystification of IKONOS! EOM 9(7), 17-21, 2000.

Toutin, Th., Chenier, R. and Carbonneau, Y., "3D geometric modelling of Ikonos Geo images". Proc. Joint ISPRS Workshop "High Resolution Mapping from Space 2001," Hannover, 19-21 September. Institute of Photogrammetry & Geoinformation, University of Hannover, 9 (on CD ROM), 2001.

Vassilopoulou, S., Hurni, L., Dietrich, V., Baltsavias, E., Pateraki, M., Lagios, E. and Parcharidis, I., "Orthophoto generation using IKONOS imagery and high-resolution DEM: a case study on volcanic hazard monitoring of Nisyros Island (Greece)". ISPRS Journal of Photogrammetry & Remote Sensing 57, 24-38, 2002.